

**Resonance meets homogenization -**  
Construction of meta-materials with astonishing  
properties

Ben Schweizer

Preprint 2016-04

October 2016

# Resonance meets homogenization – Construction of meta-materials with astonishing properties<sup>1</sup>

Ben Schweizer<sup>2</sup>

October 2016

Meta-materials are assemblies of small components. Even though the single component consists of ordinary materials, the meta-material may behave effectively in a way that is not known from ordinary materials. In this text, we discuss some meta-materials that exhibit unusual properties in the propagation of sound or light. The phenomena are based on resonance effects in the small components. The small (sub-wavelength) components can be resonant to the wave-length of an external field if they incorporate singular features such as a high contrast or a singular geometry. Homogenization theory allows to derive effective equations for the macroscopic description of the meta-material and to verify its unusual properties. We discuss three examples: Sound-absorbing materials, optical materials with a negative index of refraction, perfect transmission through grated metals.

**Key-words:** Meta-materials, resonance, homogenization, Helmholtz equation, Maxwell's equations, sound absorbers, negative index materials

**AMS-classification:** 78M40, 35B27, 35B34

## 1 Introduction

In this overview article, we discuss three meta-materials that show an interesting macroscopic behavior due to resonance effects in their microscopic elements. We start with a description of the two building blocks: resonance and homogenization.

### 1.1 Resonance

Resonance occurs in objects that have the ability to oscillate. In the case of resonance, an external field with moderate amplitude can generate large oscillations in the (resonant) object.

---

<sup>1</sup>Written for *Jahresberichte der DMV*. Appears under DOI: 10.1365/s13291-016-0153-2

<sup>2</sup>Technische Universität Dortmund, Fakultät für Mathematik, Vogelpothsweg 87, D-44227 Dortmund, Germany.

A first example is the body of a violin, see Figure 1: The air in the body can resonate, the resonance amplifies the vibrations of the string. Another example is a radio: An electric circuit consisting of a coil and a tunable capacitor can oscillate at a tunable frequency. If the right frequency is selected, the electric oscillations in an antenna can trigger oscillations in the circuit. As a last example, we mention a swing on a playground: A child on the swing moves periodically with some frequency; if it chooses the right frequency, a small periodic motion of the legs can lead to a large motion of the child.

Let us model the effect with a simple equation. We describe the state of the object at time  $t$  with the real number  $U(t)$  and assume that the time-evolution obeys the ordinary differential equation

$$\partial_t^2 U(t) = -\omega_0^2 U(t) + f(t). \quad (1)$$

We use the equation of an harmonic oscillator,  $\partial_t^2 U = -\omega_0^2 U$ , to model that the resonator has the ability to oscillate (the equation possesses the solution  $\sin(\omega_0 t)$ ). The function  $f$  models the forcing by an external field.

Let us calculate the solution for the time-harmonic forcing  $f(t) = \alpha e^{-i\omega t}$  with a frequency  $\omega \neq \omega_0$ . The ansatz  $U(t) = A e^{-i\omega t}$  yields a solution if  $-\omega^2 A + \omega_0^2 A = \alpha$ , hence the amplitude of solutions is

$$A = \frac{\alpha}{\omega_0^2 - \omega^2}. \quad (2)$$

We observe that, if the frequency  $\omega$  of the forcing is close to the resonance frequency  $\omega_0$ , the amplitude  $A$  is large compared to the amplitude  $\alpha$  of the external field. This is resonance.

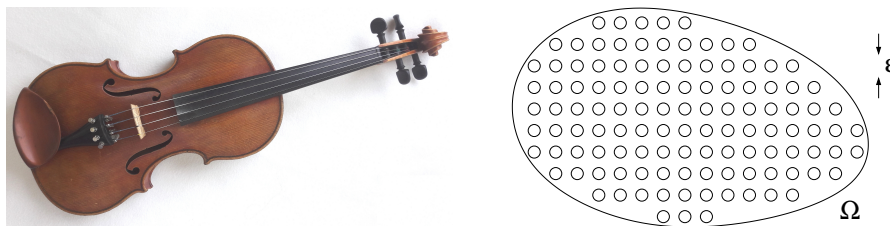


Figure 1: Left: A violin, an example for a resonator. Right: The standard setting of homogenization.

## 1.2 Homogenization

In its most elementary form, homogenization theory is concerned with the following question: Let a material be highly heterogeneous, e.g. containing many small sub-structures of size  $\varepsilon > 0$ . Let furthermore a physical process (e.g. heat conduction) be described by a partial differential equation in the medium and let  $u^\varepsilon : \Omega \rightarrow \mathbb{R}$  be the solution to this problem, see Figure 1. Then, for small

$\varepsilon > 0$ , how does  $u^\varepsilon$  look like? Or, more mathematically: Assume that, as  $\varepsilon \rightarrow 0$ , the functions  $u^\varepsilon$  converge in some topology,  $u^\varepsilon \rightarrow u$ . What is the equation that characterizes  $u$ ?

To be more specific, let us consider the wave equation  $\partial_t^2 u^\varepsilon = \nabla \cdot (a_\varepsilon \nabla u^\varepsilon)$  in a domain  $\Omega \subset \mathbb{R}^n$ . The coefficient  $a_\varepsilon$  has oscillations on the scale  $\varepsilon > 0$ , the standard choice is to set  $a_\varepsilon(x) = a(x/\varepsilon)$  for some function  $a$  which is 1-periodic in every coordinate direction. The oscillatory coefficient  $a_\varepsilon$  describes the microscopically structured material. We are interested in the effective behavior of waves in the heterogeneous medium. In order to simplify, we restrict ourselves to the analysis of a single frequency  $\omega > 0$ . Assuming that every part of the medium oscillates with this superimposed frequency, we write  $u^\varepsilon(x, t) = u^\varepsilon(x)e^{-i\omega t}$  (time-harmonic ansatz). This simplifies the wave equation to the Helmholtz problem

$$-\nabla \cdot (a_\varepsilon \nabla u^\varepsilon) = \omega^2 u^\varepsilon \quad \text{in } \Omega. \quad (3)$$

Standard homogenization theory (e.g. [1] or [22]) provides that the oscillatory coefficient  $a_\varepsilon$  can be replaced, in the limit  $\varepsilon \rightarrow 0$ , by an averaged coefficient  $a_*$ . Under very natural assumptions on  $a_\varepsilon$  and  $\omega$ , there holds  $u^\varepsilon \rightarrow u$  in  $L^2(\Omega)$  where the limit  $u$  is the unique solution of the effective problem

$$-\nabla \cdot (a_* \nabla u) = \omega^2 u \quad \text{in } \Omega. \quad (4)$$

The coefficient  $a_*$  is given by formulas that involve cell-problem solutions. Essentially, the averaged behavior of solutions to a single periodicity cell determines the behavior of the effective coefficient  $a_*$ . This implies natural bounds such as  $\|a_*\| \leq \sup_{x \in \Omega} \|a_\varepsilon(x)\|$ : The maximal conductivity of a heterogeneous medium cannot be larger than the conductivity of its constituents.

Homogenization theory started with contributions of Sanchez-Palencia and Tartar [42], the special case of periodic homogenization was greatly simplified with the notion of two-scale convergence in [1], [38]. The concepts were extended to stochastic homogenization [29], to multiple scales [3], and to measure valued limit structures [10], [20]. The method of periodic unfolding was introduced [22]; it is a slightly more geometric method than two-scale convergence, but essentially equivalent. Applications include time-dependent and nonlinear problems, high contrast problems [2], [5], spectral properties of operators [4], and long time behavior [23].

### 1.3 Resonance meets homogenization

The homogenization limit can turn out to be very different when resonance effects occur. Let us consider a situation in which each of the microscopic structures has a resonant behavior. If  $\omega$  is close to the resonant frequency  $\omega_0$ , the behavior of the single microscopic element can be extreme (e.g. with large values of the solution  $u^\varepsilon$  in the single structure). In such a case,  $a_*$  can have extreme values — values that cannot be expected from the values of  $a_\varepsilon$ .

In our first example on sound waves, we will see this effect. Standard homogenization leads from the Helmholtz equation (3) to the effective system (4). Instead, the Helmholtz equation in a more complex geometry (5) leads to the effective system (13), which unexpectedly contains the (possibly large) coefficient  $\Lambda$ .

With this very general description in mind, let us now move on and discuss specific examples. In all the examples of this overview, a key feature is the following: The single element of size  $\varepsilon$  is resonant to the frequency  $\omega_0$ . This is a nontrivial requirement, since we consider  $\varepsilon \rightarrow 0$  and keep  $\omega_0 > 0$  fixed. The property must be achieved by some singular construction, either by a large contrast or by the inclusion of small substructures in the periodicity cell.

## 2 Acoustic waves

Our first example for homogenization with resonance effects was treated only recently in mathematical terms. Nevertheless, we regard it as a prototypical example which is easy to understand in its principal ideas. We therefore do not follow historical pathways, but start with this example on sound waves.

We want to investigate sound absorbing structures. In order to damp sound waves in a room, one oftentimes uses ceilings or walls with holes in it, see Figure 2. If the single hole is resonant with the sound wave, then the sound wave induces large pressure oscillations in the hole and a large amount of energy is absorbed by friction. Let us think about the possibility of a resonance. Is it possible that an opening (with a diameter of, say, 1 cm) is in resonance with a sound wave? A sound wave at 340 Hz has a wave-length of 1 m, the highest frequencies that are audible to the human ear have a wave-length of about 17 mm. We ask: If a single standing wave does not fit into the opening, can there be resonance?

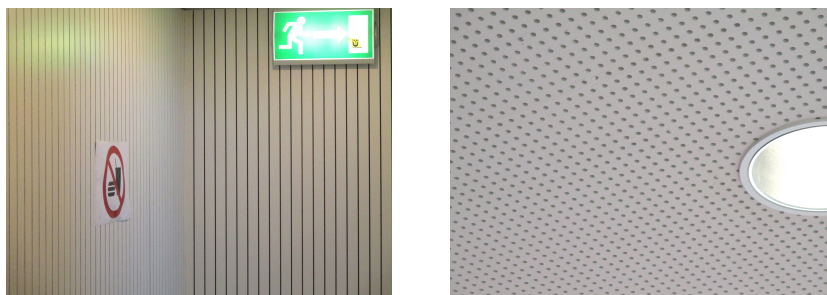


Figure 2: Sound absorbing structures used in lecture halls of the TU Dortmund.

Sound waves, i.e. pressure waves in gas, are described well by the linear wave equation. We denote by  $p = p(x, t)$  the deviation of the pressure from atmospheric pressure and by  $c > 0$  the speed of sound. Then our model for sound waves is the wave equation  $\partial_t^2 p = c^2 \Delta p$ . Using the time harmonic ansatz

$p(x, t) = u(x)e^{-i\omega t}$  and assuming  $c = 1$  (which can be obtained by a normalization of the domain), the spatial function  $u$  must solve the Helmholtz equation

$$-\Delta u^\varepsilon = \omega^2 u^\varepsilon \quad \text{in } \Omega_\varepsilon. \quad (5)$$

The small parameter  $\varepsilon > 0$  does not appear in the equation, but it may appear in the definition of the domain  $\Omega_\varepsilon \subset \mathbb{R}^n$ ; we are interested in domains that contain  $\varepsilon$ -scale substructures. Our question is: Can there appear an interesting effective equation that replaces (5) in the limit  $\varepsilon \rightarrow 0$ ? We recall that we consider  $\varepsilon \rightarrow 0$  at fixed frequency  $\omega$ , hence the structures are much smaller than the wave-length.

## 2.1 The Helmholtz resonator

At this point we want to describe a well-known resonator for sound waves: the Helmholtz resonator. We all know an example from daily life: an empty glass-bottle. If one blows over the bottle-opening, producing a low tone, one can generate oscillations in the bottle. At a specific frequency, resonance occurs and the tone is considerably amplified.

The idealized Helmholtz resonator consists of a volume  $R \subset \mathbb{R}^n$ ,  $n = 2, 3$ , (in our example the air-filled interior of the bottle), enclosed by a sound hard wall  $\Sigma \subset \mathbb{R}^n$  (the glass). It is important that the wall does not separate completely the interior from the exterior; instead, the bottle-neck leaves open a connection  $K$  between inside and outside air.

Let us think about the resonance frequency  $\omega_0$  of a Helmholtz resonator; our aim is to derive a formula for  $\omega_0$ . We will obtain the well-known expression with a mathematical construction that can actually also be transformed into a proof of the formula.

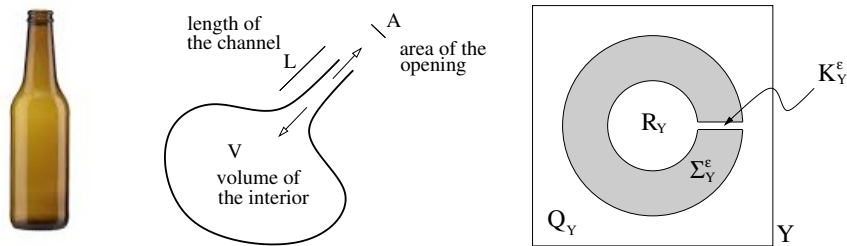


Figure 3: Left: A Helmholtz resonator from daily life experience. Middle: Explanatory sketch of a Helmholtz resonator, the arrows indicate the flow of air into and out of the volume during resonance. Right: Mathematical sketch of a periodicity cell that contains a Helmholtz resonator.

Without an external force and with trivial boundary conditions, one expects that (generically) the solution  $u^\varepsilon$  of the Helmholtz equation (5) on a bounded domain  $\Omega_\varepsilon$  vanishes. A resonant frequency is a number  $\omega > 0$  such that (5) has a nontrivial solution. Let us therefore consider the eigenvalue problem

$$-\Delta u = \lambda u \quad (6)$$

in the air volume. We want to find  $\lambda > 0$  such that (6) has a nontrivial solution  $u$ . The air volume is  $\mathbb{R}^n \setminus \Sigma$ , it consists of the interior  $R$ , the bottle-neck  $K$ , and the exterior domain. We impose Neumann boundary conditions on the boundary  $\partial\Sigma$  of the obstacle  $\Sigma$ . Regarding the eigenfunction  $u$ , our guess is that it essentially has the following shape:

$$u(x) \approx \begin{cases} 1 & \text{for } x \text{ in } R \text{ (in the bottle),} \\ 0 & \text{for } x \text{ in } \mathbb{R}^n \setminus (R \cup \Sigma \cup K). \end{cases} \quad (7)$$

The corresponding time-dependent solution describes well the physical situation: The pressure is constant outside the resonator (the pressure variations vanish). Inside the resonator, the pressure is constant in space and oscillatory in time (pressure variations are like  $\sin(\sqrt{\lambda}t)$ ).

We denote by  $\Gamma$  a cross section in the channel  $K$  and by  $A := |\Gamma|$  the measure of this cross section,  $A$  is the area of the opening. An integration over the resonator volume  $R$  with the volume  $V := |R|$  gives

$$\lambda V \approx \int_R \lambda u = - \int_R \Delta u = - \int_{\Gamma} \partial_n u \approx \frac{A}{L}. \quad (8)$$

In the first step we used that  $u$  is essentially 1 inside the resonator  $R$  with volume  $V$ . In the second step we exploited equation (6). In the third step we performed an integration by parts, using that the normal derivative of  $u$  vanishes on the boundary of  $\Sigma$ . Finally, in the last step, we used a geometric fact: When  $u$  decreases from 1 to 0 on the way from the interior  $R$  to the exterior, then the typical gradient of  $u$  in the channel  $K$  is  $\nabla u \approx -L^{-1}n$ , where  $L$  is the length of the channel and  $n$  a normalized vector that points in the long direction of the channel and towards the exterior domain. Accordingly,  $\partial_n u = n \cdot \nabla u \approx -L^{-1}$ . The integration provides the factor  $A = |\Gamma|$ . The calculation (8) yields the desired formula for the resonance frequency:

$$\omega = \sqrt{\lambda} \approx \sqrt{\frac{A}{LV}}. \quad (9)$$

We recall that  $A$  is the opening area,  $V$  the volume of the resonator, and  $L$  the length of the channel.

## 2.2 A mathematical property of a single small Helmholtz resonator

The formula (9) has a special property that we will exploit in the following: It is true that a smaller volume  $V$  of the resonator results in a higher frequency — which seems to make it difficult to have smaller and smaller resonators for a fixed frequency. But the mechanism can be compensated: We may construct small objects with a small volume  $V$  and a small length  $L$ , but with, at the same

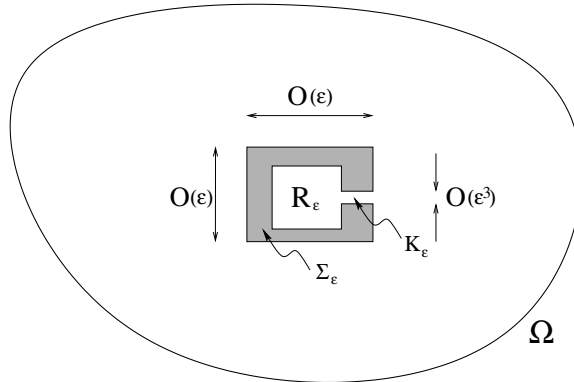


Figure 4: A two-dimensional domain with an inclusion of size  $\varepsilon > 0$ . The inclusion has a singular geometry in the sense that the channel  $K_\varepsilon$  is thin in comparison to the object  $\Sigma_\varepsilon$ . We are interested in the spectrum of the Laplace operator on the domain  $\Omega_\varepsilon = \Omega \setminus \Sigma_\varepsilon$ .

time, very small values of  $A$ . Doing so, we can construct a sequence of smaller and smaller structures that all have the same frequency  $\omega_0$ .

The observation that such singular structures may give rise to nontrivial spectral properties is quite old. A very influential article with mathematical results was written by Beale in 1973 [6]. Beale investigated the exterior problem of a cavity of fixed size, but with a very thin channel that connects interior and exterior domain. Similarly, in [17] an object of order 1 with a thin connecting tube is considered and spectral properties together with convergence rates are analyzed. Similar problems are considered (with a less mathematical language) in [26], [27], [30], and [31]. Related results are available also for elastic models, see e.g. [25].

We describe here a mathematical theorem that is formulated and proved in [43]: Let  $\Omega_\varepsilon = \Omega \setminus \Sigma_\varepsilon \subset \mathbb{R}^2$  be as sketched in Figure 4. In particular,  $\Sigma_\varepsilon$  has a diameter of order  $\varepsilon$ , the interior  $R_\varepsilon$  has a volume of order  $|R_\varepsilon| = O(\varepsilon^2)$ . Furthermore, the channel  $K_\varepsilon$  with length  $L_\varepsilon$  is very thin: Its cross-section  $\Gamma_\varepsilon$  has an area  $|\Gamma_\varepsilon|$  such that the limit

$$\mu_0 = \lim_{\varepsilon \rightarrow 0} \frac{L_\varepsilon |R_\varepsilon|}{|\Gamma_\varepsilon|} \quad (10)$$

exists. Let  $T_\varepsilon := (-\Delta)^{-1}$  on  $L^2(\Omega_\varepsilon)$  be the solution operator for the Poisson problem with homogeneous Neumann boundary conditions on  $\partial\Sigma_\varepsilon$  and homogeneous Dirichlet conditions on  $\partial\Omega$ . Then, for every cut-off parameter  $\delta > 0$ , the spectrum  $\sigma(T_\varepsilon)$  of  $T_\varepsilon$  satisfies

$$\mathbb{C} \supset \sigma(T_\varepsilon) \setminus B_\delta(0) = \{\mu_\varepsilon, \lambda_1^\varepsilon, \lambda_2^\varepsilon, \dots, \lambda_N^\varepsilon\}, \quad (11)$$

and the first eigenvalue satisfies  $\mu_\varepsilon \rightarrow \mu_0$ , where  $\mu_0$  is given by (10). The other eigenvalues are perturbations of the eigenvalues of  $(-\Delta)^{-1}$  on  $\Omega$  (without an



obstacle):  $\lambda_k^\varepsilon \rightarrow \lambda_k$  as  $\varepsilon \rightarrow 0$  (for every index  $1 \leq k \leq N$ ), where  $(\lambda_k)_k$  are the ordered Dirichlet eigenvalues of  $-(\Delta)^{-1}$  on  $\Omega$ . We assumed here that the limiting resonant eigenvalue  $\mu_0$  is larger than the largest Dirichlet eigenvalue  $\lambda_1$  on  $\Omega$ . The result can also be shown in  $\mathbb{R}^3$ . It gives a precise description of the fact that a small object can have a resonant frequency of order 1.

## 2.3 Homogenization: Many small resonators

At this point, we have found a sequence of small structures that have a fixed resonance frequency  $\omega_0$ . We can therefore distribute many of these structures (a number of order  $\varepsilon^{-n}$  where  $n$  is the space dimension). We ask: If we distribute the  $\varepsilon$ -size structures in a subregion  $D \subset \Omega$  of our macroscopic domain  $\Omega$ , what is the effective behavior of the meta-material in  $D$ ?

Let us describe our question in a more mathematical language: We consider a domain  $\Omega_\varepsilon \subset \mathbb{R}^n$ ,  $n = 2$  or  $n = 3$ , which is obtained by removing  $O(\varepsilon^{-n})$  small obstacles of typical size  $\varepsilon > 0$  from a domain  $\Omega \subset \mathbb{R}^n$ . For a fixed frequency  $\omega \in \mathbb{R}$ , we study solutions  $u^\varepsilon \in H^1(\Omega_\varepsilon)$  to the Helmholtz equation

$$\begin{aligned} -\Delta u^\varepsilon &= \omega^2 u^\varepsilon && \text{in } \Omega_\varepsilon, \\ \partial_n u^\varepsilon &= 0 && \text{on } \partial\Omega_\varepsilon \setminus \partial\Omega, \\ u^\varepsilon &= g && \text{on } \partial\Omega. \end{aligned} \tag{12}$$

With the boundary condition  $g \in H^1(\Omega)$  we enforce that solutions are nontrivial. Assume that  $v$  is a limit of  $u^\varepsilon$  as  $\varepsilon \rightarrow 0$  in some appropriate sense. What is the equation for  $v$  in the domain  $\Omega$ ?

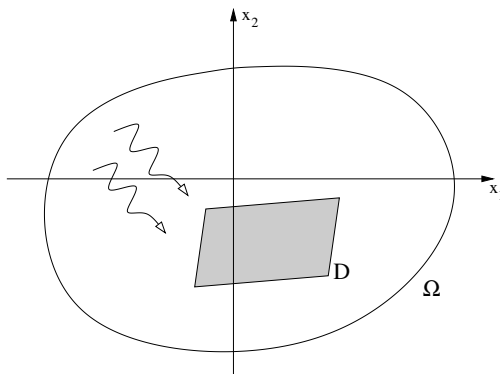


Figure 5: Geometry of the homogenized system. The limit  $v$  is described by the Helmholtz equation (13) in  $\Omega$ . The coefficients  $A_*$  and  $\Lambda$  of the limit problem (i.e. the effective coefficients) are constant in  $\Omega \setminus D$  and in  $D$ . In the meta-material region  $D$ , which contains the small-scale structures for finite  $\varepsilon > 0$ , coefficients can be large and/or negative.

The mathematical result of [34] is the following effective equation:

$$-\nabla \cdot (A_* \nabla v) = \omega^2 \Lambda v \quad \text{in } \Omega, \tag{13}$$

with the unchanged boundary condition  $v = g$  on  $\partial\Omega$ . The function  $v : \Omega \rightarrow \mathbb{R}$  is the weak limit of  $u^\varepsilon$ , but only in  $\Omega \setminus D$ . In  $D$ , the function  $v$  represents the typical values of  $u^\varepsilon$  *outside* the small Helmholtz resonators (more precisely:  $v(x)$  is the value of the two-scale limit  $u_0(x, y)$  of  $u^\varepsilon$  for points  $y$  outside the resonator region). The effective coefficient  $A_*$  on the left hand side is the same as in classical homogenization results, i.e. as for micro-structures without resonance, compare (4). When we write a formula for  $A_*$ , we must distinguish between the subset  $D \subset \Omega$  that contains the resonators, and the rest (cp. Figure 5). We have  $A_*(x) = 1$  for  $x \in \Omega \setminus D$  and  $A_*(x) = A_{\text{eff}}$  for  $x \in D$ , where  $A_{\text{eff}} \in \mathbb{R}^{n \times n}$  is given by cell-problems. The formulas show that  $A_{\text{eff}}$  is frequency independent, no large and no negative values can occur.

The interesting contribution in the effective system (13) is the parameter  $\Lambda \in \mathbb{R}$ . It is shown in [34] that  $\Lambda(x) = 1$  for  $x \in \Omega \setminus D$  and  $\Lambda(x) = \Lambda_{\text{eff}}$  for  $x \in D$ . If the single inclusion has the volume  $V\varepsilon^n$ , the channel length  $L\varepsilon$ , and the opening area  $A\varepsilon^{n+1}$ , then the real number  $\Lambda_{\text{eff}}$  is given by

$$\Lambda_{\text{eff}} := Q - \frac{A}{L} \left( \omega^2 - \frac{A}{LV} \right)^{-1}, \quad (14)$$

where  $Q$  is the volume in the single periodicity cell outside the resonator.

Formula (14) provides the quantitative description of the microscopic resonance: The effective parameter  $\Lambda_{\text{eff}}$  is frequency dependent; in this sense,  $D$  is a dispersive medium. Furthermore, upon varying the frequency  $\omega$  of the wave, the parameter  $\Lambda_{\text{eff}}$  can have large values and negative values. This special behavior occurs for  $\omega$  close to the resonance frequency  $\sqrt{A/(LV)}$ . We stress that there is a similarity of the algebraic expressions in (14) and in the amplitude formula (2) of the introduction (both containing a denominator  $\omega^2 - \omega_0^2$ ).

### 3 Electromagnetic waves

Sound was our first example for resonances in a meta-material. We now move on and discuss light, which is more interesting for applications. The study of resonance effects for light is also mathematically older. This is true, even though the equations for the description of light are more challenging than the wave equation. It is for this latter reason that we postponed the description of light in heterogeneous media to this point. Following standard notations, we will denote the small parameter from now on by  $\eta > 0$ .

#### 3.1 Homogenization of Maxwell's equations

Electromagnetic waves in a domain  $\Omega \subset \mathbb{R}^3$  are described by two fields  $E^\eta, H^\eta : \Omega \rightarrow \mathbb{C}^3$ . The fields must solve Maxwell's equations. In the time-harmonic

framework with the time dependence  $e^{-i\omega t}$ , Maxwell's equations read

$$\operatorname{curl} E^\eta = i\omega\mu_0 H^\eta, \quad (15)$$

$$\operatorname{curl} H^\eta = -i\omega\varepsilon_\eta\varepsilon_0 E^\eta, \quad (16)$$

they must be solved in  $\Omega$ . The equations involve two material parameters, a permeability  $\mu$  and a permittivity  $\varepsilon$ . The permeability is almost the same for all materials, we therefore write the first equation with the coefficient  $\mu_0$ , the permeability of vacuum, a positive real number. In contrast, the permittivity is different for different materials and we therefore write  $\varepsilon_\eta\varepsilon_0$  for the coefficient in the second equation. Here,  $\varepsilon_0$  is the permittivity of vacuum and  $\varepsilon_\eta$  is the relative permittivity of the medium. Given the coefficient  $\varepsilon_\eta : \Omega \rightarrow \mathbb{C}$  which describes the material properties in the domain  $\Omega$ , the system (15)–(16) determines the fields  $(E^\eta, H^\eta)$ .

In Maxwell's equations, the symbol for the permittivity is always  $\varepsilon$ . We therefore use here  $\eta > 0$  as the small parameter that indicates the size of small structures. To distribute small structures in the domain  $\Omega$  means nothing else than to prescribe a sequence of coefficient functions  $\varepsilon_\eta : \Omega \rightarrow \mathbb{C}$ .

Our aim is to analyze the behavior of solutions  $(E^\eta, H^\eta)$  of (15)–(16) in the limit  $\eta \rightarrow 0$ . The wish is to follow the derivation of (13) from (12) and to obtain that limit fields satisfy an effective system with frequency dependent coefficients. In fact, something similar can be shown — at least if the limit fields  $(\hat{E}, \hat{H})$  are defined with an appropriate limiting procedure from the sequence  $(E^\eta, H^\eta)$ : For piecewise constant parameter functions  $\hat{\mu}$  and  $\hat{\varepsilon}$ , the limit fields  $(\hat{E}, \hat{H})$  solve in  $\Omega$  the system

$$\operatorname{curl} \hat{E} = i\omega\mu_0\hat{\mu}\hat{H}, \quad (17)$$

$$\operatorname{curl} \hat{H} = -i\omega\varepsilon_0\hat{\varepsilon}\hat{E}. \quad (18)$$

In standard homogenization settings with periodic and bounded coefficients  $\varepsilon_\eta(x) = \varepsilon_0(x, x/\eta)$ , it is easy to derive the effective system (17)–(18) for some effective coefficient  $\hat{\varepsilon}$ . Unfortunately, only the trivial coefficient  $\hat{\mu} = 1$  will appear in the standard setting, and the coefficient  $\hat{\varepsilon}$  will be bounded by the bounds on  $\varepsilon_0$ . Compare e.g. [29], where also the case of small (non-resonant, perfectly conducting) inclusions is treated. In the case with inclusions, a value  $\hat{\mu} \neq 1$  can be achieved, but  $\hat{\mu}$  respects the natural bounds and is, in particular, always positive.

Our aim in Maxwell's equations is to use resonant micro-structures in order to obtain nontrivial effective equations (17)–(18).

### 3.2 Nontrivial limits: observed as announced

In natural materials, electromagnetic waves are described by a system such as (17)–(18) with some coefficients  $\hat{\varepsilon}$  and  $\hat{\mu}$ . Essentially, the parameter  $\hat{\mu} = 1$

is observed,  $\hat{\epsilon}$  can be complex, it can even have a negative real part, but the imaginary part is always non-negative. The Maxwell system has the property that wave-like solutions exist only if the product  $\hat{\mu}\hat{\epsilon}$  is positive. For natural materials with  $\hat{\mu} = 1$ , we only have two possibilities: If  $\hat{\epsilon}$  is positive, waves can travel through the medium, if  $\hat{\epsilon}$  is negative, the medium is opaque.

In 1968, Veselago performed theoretical studies on (17)–(18) assuming that both  $\hat{\mu}$  and  $\hat{\epsilon}$  are negative (a negative index material, [46]). In negative index materials, wave-like solutions exist and hence light can propagate. Interesting effects occur at the interfaces between ordinary materials and negative index materials. One example is negative refraction as indicated in Figure 6.

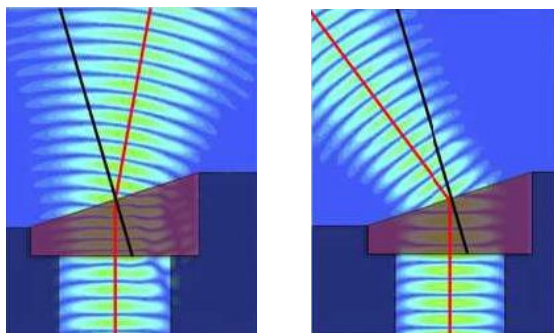


Figure 6: Computation of positive/negative refraction for a positive/negative index prism. Image from J.B. Pendry et al., *Physics Today* 57, 6, 37 (2004), with the permission of the American Institute of Physics.

Since negative index materials cannot be found in nature, the work of Veselago did not receive much attention until about 2000. Around that year, Pendry, Smith and various co-workers made two major discoveries that boosted the investigation of negative index materials. (i) A meta-material was suggested that acts, effectively, as a negative index materials. The meta-material was actually also realized and experimental data confirmed the negative index property [44]. (ii) The astonishing imaging properties of a negative index material were discovered [40]. See also [39] and [45].

### 3.3 Mathematical homogenization of wires, split rings, and Mie resonators

At this point, mathematics was challenged! There was a construction of a negative index meta-material. In mathematical terms: There was the suggestion of a sequence of permittivity coefficient functions  $\varepsilon_\eta = \varepsilon_\eta(x)$  such that the corresponding medium behaves, effectively, like a negative index material. In other words: There was experimental evidence that fields  $(E^\eta, H^\eta)$  solving (15)–(16) behave, for small values of  $\eta$ , like solutions  $(\hat{E}, \hat{H})$  to (17)–(18) with negative coefficients  $\hat{\mu}$  and  $\hat{\epsilon}$ . Can this limit behavior be derived with homogenization theory?

### 3.3.1 Wire structures

The first mathematical homogenization results for resonant structures have been obtained for wires. The main reason is that Maxwell's equations simplify in this case. Let us assume that both the geometry and the fields are independent of the  $x_3$ -direction (hence the wires extend in the  $x_3$  direction). Let us assume additionally that the magnetic field is aligned with the wires,  $H(x_1, x_2, x_3) = u(x_1, x_2)e_3$ . In this situation, Maxwell's equations reduce to a two-dimensional Helmholtz equation for the scalar variable  $u$ . It was certainly also helpful that wires had already been analyzed in the context of elasticity, see e.g. [7], [8]. For a result in the frame-work of heat conduction see [21].

A domain with straight wires can be constructed with the usual periodic repetition of a periodicity cube. The cube must contain a cylinder that is aligned with an edge and that connects opposite walls of the cube, see Figure 8. We emphasize that, in such a construction, the cylinder (i.e. the inclusion) is not compactly contained in the open unit cell. This means that some standard homogenization methods cannot be applied. Indeed, the fact that the wires form macroscopic objects can lead to interesting effects such as non-locality of the effective equation.

With this background, Bouchitté and co-workers were able to obtain interesting results for Maxwell's equations in wire structures: a negative effective permittivity  $\varepsilon$  in [24], nonlocal effective equations in [14], and an effective magnetic response in [11]. As another example for a reduced model that allowed a mathematical analysis, we mention [32].

### 3.3.2 Split ring structures

The first mathematical analysis of a truly three-dimensional structure was carried out in [15] (we remark that the results of [15] are older than those of [9]). The setting was designed to resemble the experimental set-up. It was shown that the periodic split ring structure can lead to a negative effective permeability  $\mu_{\text{eff}}$ . The key mechanism is the resonance of the split ring with the frequency  $\omega$  of the external field. This is our main example for homogenization with resonance, we therefore want to describe the mathematical analysis of this problem in some more detail.

We recall that we analyze solutions  $(E^\eta, H^\eta)$  to (15)–(16). Since we use only non-magnetic materials, the only quantity that remains to be specified is the permittivity  $\varepsilon_\eta$ . We want to describe a split-ring geometry, which can be done in the following three steps. (1) We consider a full torus  $T \subset Y = (0, 1)^3$  in the unit cell, not touching the boundaries of the cell. By removing a thin slice  $S_Y^\eta$  (the slit) from the full torus  $T$ , we obtain the *split ring*  $\Sigma_Y^\eta := T \setminus S_Y^\eta$  (cp. Figure 7). We observe that the full torus  $T$  is not simply connected, but the split ring  $\Sigma_Y^\eta$  is simply connected. (2) A set  $\Sigma_\eta \subset D \subset \Omega$  in the macroscopic domain is constructed as the union over the scaled and shifted split rings  $\eta(k + \Sigma_Y^\eta)$ , the

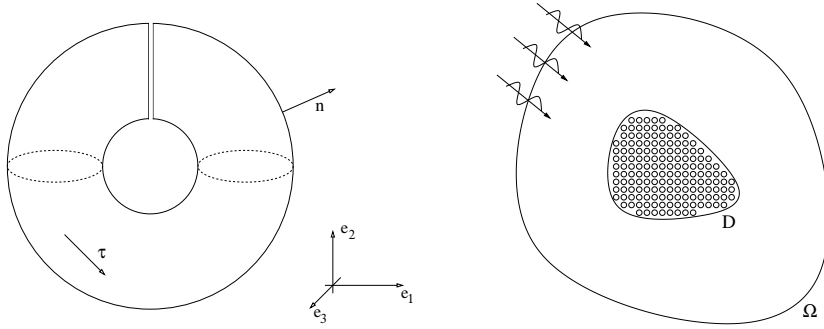


Figure 7: Left: A single split ring, constructed from a full torus with size of order 1 by removing a thin region of width  $\eta^2$ . Right: Many (a number of order  $\eta^{-3}$ ) scaled full tori of typical diameter  $\eta$  are periodically distributed in a region  $D \subset \Omega$ . This geometrical construction determines the coefficient  $\varepsilon_\eta$ . We are interested in the behavior of solutions  $(E^\eta, H^\eta)$  of (15)–(16) for this complex coefficient.

union is taken over all  $k$  such that the whole cube  $\eta(k + Y)$  is contained in  $D$ . (3) With a conductivity constant  $\kappa > 0$ , the material parameter  $\varepsilon_\eta : \mathbb{R}^3 \rightarrow \mathbb{C}$  is

$$\varepsilon_\eta = \begin{cases} 1 + i\frac{\kappa}{\eta^2} & \text{in the rings ,} \\ 1 & \text{else .} \end{cases} \quad (19)$$

We note that the small parameter  $\eta > 0$  appears at several points of the construction: (a) the size of the microstructure is  $\eta$ , the number of small full tori in the domain is of the order  $\eta^{-3}$ ; (b) the slits of the rings in the physical domain have only the width  $2\alpha\eta^3$ ; (c) the conductivity in the rings is high, it behaves like  $\kappa\eta^{-2}$ . We ask:

Let the coefficient  $\varepsilon_\eta$  be as in (19) and let  $(E^\eta, H^\eta)$  be a bounded sequence of solutions to (15)–(16). Can we associate to the sequence some limiting fields  $(\hat{E}, \hat{H})$  that solve (17)–(18)? What are the effective coefficients  $\hat{\mu}$  and  $\hat{\varepsilon}$  of the limit system?

Since we assume that  $(E^\eta, H^\eta)$  is a bounded sequence in  $L^2(\Omega)$ , we find, for an appropriate subsequence  $\eta \rightarrow 0$ , a weak limit  $(E, H)$ . In equation (15), we can take the distributional limit and conclude that  $(E, H)$  satisfies the equation (17) with  $\hat{\mu} = 1$ . This observation worries us, since it suggests that no magnetic activity can be observed. But we can resolve this problem as follows: The limiting field  $\hat{H}$  is *not* the weak limit of the sequence  $H^\eta$ , but it is obtained by another limit process. Indeed,  $\hat{H}$  is what we call today the *geometric limit*. Denoting by  $\hat{\mu}$  the tensor that relates the two limit fields,  $H = \hat{\mu}\hat{H}$ , and setting  $\hat{E} = E$ , we obtain the effective equation (17) by definition.

To consider the geometric limit  $\hat{H}$  of the sequence  $H^\eta$  turns out to be the right concept. The *geometric average* of a two-scale limit was introduced in [9],

the geometric average of the two-scale limit is the *geometric limit*. Essentially, we define  $\hat{H}$  as the limit of *line integrals* over  $H^\eta$ . In this sense,  $\hat{H}$  is the typical value of  $H^\eta$  *outside of the rings*, since line integrals are evaluated only for curves that do not pass through the ring. In fact, with this geometric concept, also the magnetic Maxwell equation (18) is not difficult to obtain. The permittivity parameter  $\hat{\varepsilon}$  is 1 outside  $D$  (since there is no micro-structure), it is  $\varepsilon_{\text{eff}}$  for an effective permittivity tensor  $\varepsilon_{\text{eff}} \in \mathbb{R}^{n \times n}$  that is determined in a classical way by cell-problems (no large and no negative values).

**Calculation of the coefficient  $\hat{\mu}$ .** Resonance effects are relevant in the remaining step of the analysis, the calculation of the tensor  $\hat{\mu}$ . We recall that  $\hat{\mu}$  quantifies the relation between the magnetic field  $H$  (obtained as an average) and the typical field  $\hat{H}$  outside the rings (obtained as the geometric limit). There holds  $\hat{\mu}(x) = 1$  for  $x \in \Omega \setminus D$  and  $\hat{\mu}(x) = \mu_{\text{eff}}$  for  $x \in D$  for some effective permeability  $\mu_{\text{eff}}$ .

Interesting formulas for  $\mu_{\text{eff}}$  can occur due to resonance effects, which have their counterpart in an interesting topological limit behavior: For positive  $\eta > 0$ , every ring has a slit and is therefore a simply connected object. Instead, in the limit  $\eta \rightarrow 0$ , the slit vanishes and the (rescaled) limit object is a closed ring. The limit object is topologically a full torus and no longer simply connected.

The microscopic structure of the magnetic field  $H^\eta$  is studied with the two-scale limit of the sequence. Compactness of  $L^2$ -bounded sequences implies that we can assume for some limit function  $H_0 = H_0(x, y)$  the convergence  $H^\eta \rightharpoonup H_0$ , with weak two-scale convergence as  $\eta \rightarrow 0$ . The two-scale limit  $H_0$  depends on the macroscopic position  $x \in \Omega$  and on  $y \in Y$ , where  $Y = [0, 1]^n$  is the periodicity cell. Similarly, we find a two-scale limit  $E_0$  of the electrical fields. Standard arguments show that  $H_0$  solves a cell-problem. As a solution,  $H_0$  can be written as a linear combination of *shape functions*, normalized solutions of the cell problem. In a standard homogenization problem in 3 dimensions, the solution space to the cell-problem is 3-dimensional, and one can typically choose three cell solutions  $H^1(y), H^2(y), H^3(y)$  with averages  $\int_Y H^k = e_k$  for  $k = 1, 2, 3$ . The same would be possible here, if the closed ring was simply connected. Instead, in our setting, the cell-problem has an extra dimension, spanned by a solution  $H^0 : Y \rightarrow \mathbb{C}^3$  with vanishing average. This vector field  $H^0$  points through the ring: In average, it points in positive  $e_3$ -direction in the hole of the closed ring, and it points in negative  $e_3$ -direction outside the ring. With this additional shape function, we can write  $H_0(x, y)$  as a linear combination,

$$H_0(x, y) = h_0(x)H^0(y) + \sum_{k=1}^3 h_k(x)H^k(y). \quad (20)$$

Loosely speaking, (20) should be read as follows: The fields  $H^k$ ,  $k = 1, 2, 3$ , are perturbations of the constant fields  $e_k$ . Hence, macroscopically and in terms of volume averages,  $H^\eta$  is comparable to  $(h_1, h_2, h_3)$ . Indeed, the weak limit of

$H^n$  coincides with this vector,  $H(x) = (h_1, h_2, h_3)(x)$ . But there is also the extra field  $H^0$ . The factor  $h_0(x)$  measures how much of this field (the microscopic field pointing through the ring) is generated at a macroscopic position  $x$ .

Resonance makes the following possible: The magnetic field average may be  $e_3$ , hence  $h_3(x) = 1$  and  $H(x) = e_3$ . But, due to induction, there also appears a magnetic field around the ring. Usually, this is a field that partially cancels the magnetic field. Here, due to resonance of the ring, also the opposite magnetic field may appear: the field in the ring may be amplified, e.g. with  $h_0(x) = 1$ . This extra field may cancel magnetic field line integrals outside the ring such that  $\hat{H} \approx 0$ . Because of  $H = \hat{\mu}\hat{H}$ , this means that large values of  $\hat{\mu} = \mu_{\text{eff}}$  can appear.

It remains to quantify how strongly  $H^0$  is triggered in the medium. This is the aim of the ‘‘slit analysis’’. Indeed, the information on how strong the extra magnetic field is triggered must come from an analysis of the *split* ring, the ring for  $\eta > 0$ . The slit analysis provides a formula for a number  $\lambda$ , which is a measure for  $h_0$  in terms of  $h_3$ :

$$\lambda(\omega, \kappa) = \frac{\varepsilon_0 \mu_0 \omega^2 D_3(\omega, \kappa)}{\varepsilon_0 \mu_0 \omega^2 |D_0(\omega, \kappa)| - \alpha (\pi \rho)^{-1} + i \kappa^{-1}}. \quad (21)$$

In this formula,  $\varepsilon_0, \mu_0, \kappa, \omega$  are the physical constants of the problem,  $\alpha, \rho$  are geometrical constants of the split rings,  $D_0, D_3$  are numbers that are obtained from cell-problems. We recognize a structure that we already know from the previous examples: for large conductivity  $\kappa$ , the imaginary term in the denominator is small. Assuming that  $D_0$  is not frequency dependent (which is true in some limit), the other two terms of the denominator are, up to multiplicative constants, of the form  $\omega^2 - \omega_0^2$ .

The fact that  $\lambda$  can be large and can have arbitrary sign implies that the same is true for  $\hat{\mu}$ , the effective permeability. Similar result have been obtained later also for flat rings of arbitrary shape, see [33]. In an analysis of perfectly conducting split rings some arguments can actually be simplified [36].

### 3.3.3 Mie resonators and combinations with wires

Split rings were the first sub-wavelength resonators that showed the negative effective permeability  $\mu_{\text{eff}}$  in experiments. Their analysis is quite intricate, but, if we insist that only materials with bounded  $\text{Re } \varepsilon_\eta$  are used, they are still the only construction for which a mathematical analysis provides the negative  $\mu_{\text{eff}}$ . The situation is different if we allow arbitrary permittivities  $\varepsilon_\eta$ . In that case, there is a simpler construction that provides a negative  $\mu_{\text{eff}}$  on the basis of Mie resonance.

Essentially, we can choose arbitrarily a shape  $\Sigma \subset Y$  (an open set, compactly contained in the open unit cell), and use it as resonator. As in the previously discussed applications, we scale the object  $\Sigma$  by  $\eta > 0$  and repeat it periodically, setting  $\Sigma_\eta = \bigcup_k \eta(k + \Sigma)$ . In order to create resonances, we choose the relative



permittivity  $\varepsilon_\eta(x) = 1$  for  $x \notin \Sigma_\eta$  and  $\varepsilon_\eta(x) = \varepsilon_r \eta^{-2}$  for  $x \in \Sigma_\eta$ , where  $\varepsilon_r \in \mathbb{C}$  is an arbitrary number with non-negative imaginary part.

This medium with dielectric resonators has been introduced and analyzed mathematically in [9]. If  $\varepsilon_r \omega^2 \in \mathbb{C}$  is close to an eigenvalue of the Dirichlet Laplace operator on the domain  $\Sigma$ , a resonance can occur in the small inclusion. The resonance can lead to a magnetic response which works, loosely speaking, as follows: It is possible that the magnetic field outside the single inclusion  $\eta(k + \Sigma)$  is essentially, say,  $e_3$ . This means that the geometric average is  $\hat{H} \approx e_3$ . But, for this boundary condition, the magnetic field in the inclusion may be pointing, in average, in the negative  $e_3$  direction. For strong resonance, we might observe the averaged field, e.g.,  $H = -10e_3$ . Because of  $H = \hat{\mu}\hat{H}$ , this implies that  $\hat{\mu}$  is negative and large in absolute value.

We emphasize that the knowledge of the Mie resonance effect and also its potential to construct negative index meta-materials was known much before [9], see e.g. [28]. Its mathematical analysis began, as already sketched above, with periodic media consisting of rods, i.e. in cases where the time-harmonic Maxwell's equations reduce to the Helmholtz equation (3). The homogenization of this problem was performed already in [11], [12], [13], [24]. In [11], the effective magnetic response is derived for the rod geometry. We note that, in this approach with resonant dielectric inclusions, a negative  $\mu_{\text{eff}}$  can be obtained without any subscale variations of the periodic geometry. For another negative index material obtained from a wire construction see [19].

**Combination with wires.** The above discussion dealt only with an interesting effective permeability  $\mu_{\text{eff}}$ . For a negative index material, we need both: negative  $\mu_{\text{eff}}$  and negative  $\varepsilon_{\text{eff}}$ . The emphasis was always on the first, since natural material can have negative  $\text{Re } \varepsilon$ . It hence should be possible to construct a negative index material from the two materials above (a negative  $\mu_{\text{eff}}$  material and a negative  $\varepsilon_{\text{eff}}$  material). Indeed, this is possible with a fine mixture of such materials; this was shown in [37].

Since a fine mixture of meta-materials is not realistic for experiments, our aim in [35] was to construct a periodic medium that realizes negative  $\mu_{\text{eff}}$  and negative  $\varepsilon_{\text{eff}}$  in one step, ideally mimicking the experimental set-up. The analysis of [35] is concerned with a geometry where wires with negative  $\varepsilon_\eta$  are combined with magnetic resonators. The model uses  $\varepsilon_\eta = \varepsilon_W \eta^{-2}$  for some  $\varepsilon_W \in \mathbb{C}$  in the wires. Furthermore, the wires are thin, with relative radius  $\gamma\eta$ , which means that they are invisible for the magnetic problem in the limit  $\eta \rightarrow 0$ . We note that it is physically desirable to have thin wires in order to have small losses in the meta-material.

The result of [35] for a geometry combining magnetic resonators with wires as in Figure 8 is the effective system (17)–(18) with  $\hat{\mu}(x) = \mu_{\text{eff}}$  and  $\hat{\varepsilon}(x) = \varepsilon_{\text{eff}}$  for  $x \in D$ , where the material parameters are

$$\mu_{\text{eff}} = \mu_{\text{eff},R} \quad \text{and} \quad \varepsilon_{\text{eff}} = \varepsilon_{\text{eff},R} + \pi\gamma^2 \varepsilon_W. \quad (22)$$

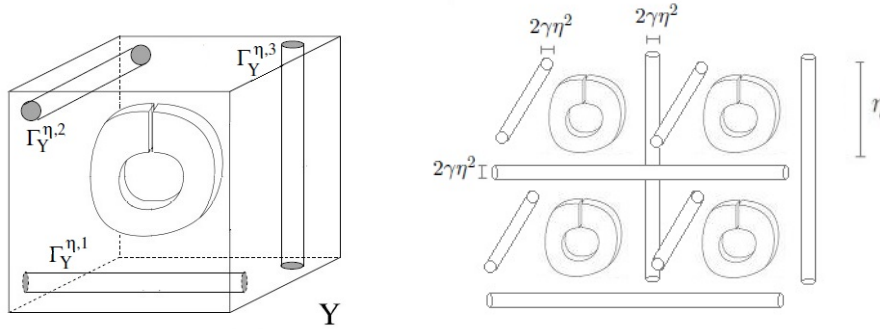


Figure 8: Thin split rings and wires. The periodic repetition of the unit cell leads to long wire elements of macroscopic length scale.

The magnetic response  $\mu_{\text{eff}}$  is exactly as in the case without wires, denoted as  $\mu_{\text{eff},R}$ . Instead, the electric response  $\varepsilon_{\text{eff}}$  does not coincide with  $\varepsilon_{\text{eff},R}$  (the effective permittivity in the absence of wires), but it receives an additive contribution from the wires. If  $\varepsilon_W$  has a negative real part and the radial parameter  $\gamma$  of the wires is sufficiently large, then  $\varepsilon_{\text{eff}}$  has a negative real part. The mathematical result reads as follows: If  $(H^\eta, E^\eta)$  solve Maxwell's equations and  $(H^\eta, E^\eta)$  converge to  $(\hat{H}, \hat{E})$  *geometrically*, then the limit fields  $(\hat{H}, \hat{E})$  solve Maxwell's equations with the effective coefficients of (22).

In the analysis of the wire structure we observe once more a topological effect: Assume that we distribute inclusions with negative  $\varepsilon$  in such a way that their relative volume vanishes and such that the inclusions do not touch the boundary of the unit cell. In such a case, due to vanishing capacity of the wires, no contribution of the inclusions is visible in the effective equations, i.e.  $\varepsilon_{\text{eff}} = \varepsilon_{\text{eff},R}$ . Instead, since in the above construction the wires are long (the complement of the wires in the periodicity cell is not simply connected), a nontrivial contribution is possible even though the wires have a vanishing capacity.

## 4 Perfect transmission

Let us start once more with an astonishing physical observation regarding light propagation: We consider a silver foil, i.e. a thin sheet of silver. Silver is opaque: If light hits a horizontal silver foil from above, the light is reflected; no light is transmitted through the foil. Let now the same foil be prepared with a grating: a periodic pattern of thin slits (channels) is cut in the foil. These channels have a width below the wave-length of light, hence, in classical approximations, one expects that the foil is still opaque. Instead, it is observed that at certain (resonant?) frequencies of light, a large proportion of the light is transmitted through the prepared foil [18], [41].

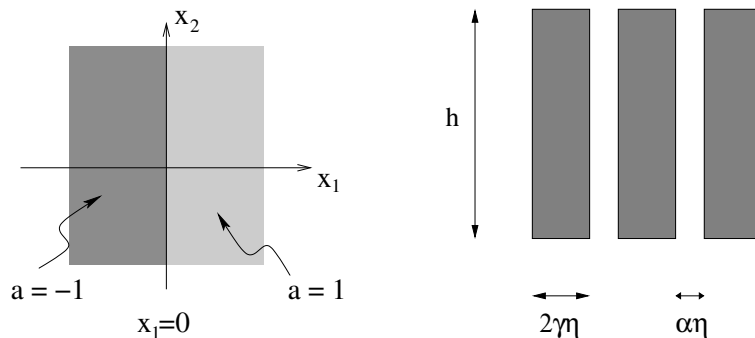


Figure 9: Two geometries with interfaces. Left: The geometry of the surface wave problem. A single interface separates media with  $a = \pm 1$ . Right: The micro-structure of the foil with grating.

## 4.1 Surface waves

It was suggested that surface waves are responsible for the experimental result. Interesting is the discussion on how surface waves might produce the effect: Via waves on the top surface of the foil or via waves along the channel walls? Regarding this discussion, we refer to [18] and note that already the title of this publication from 2002 expresses the controversial discussion.

Let us start by explaining in mathematical language surface waves (or surface plasmons). To simplify as much as possible, we consider the Helmholtz equation at vanishing frequency  $\omega = 0$ ,

$$-\nabla \cdot (a(x)\nabla u(x)) = 0. \quad (23)$$

Let us assume that the coefficient  $a = a(x_1, x_2)$  of the two-dimensional problem is given by the geometry that is indicated in Figure 9:  $a(x_1, x_2) = 1$  for  $x_1 > 0$  and  $a(x_1, x_2) = -1$  for  $x_1 < 0$ . In this setting, a solution to equation (23) is given by

$$u(x_1, x_2) = \exp(-k|x_1|) \sin(kx_2),$$

where  $k > 0$  is an arbitrary number. Indeed,  $u$  is harmonic on the left and on the right domain, it is continuous across the interface, and the quantity  $e_1 \cdot (a(x)\nabla u(x))$  is also continuous. Since the solution decays exponentially away from the interface, we may say that  $u$  is localized to the surface. At small frequencies  $\omega$ , there exist solutions to the Helmholtz equation with similar shape. With the time dependence  $e^{-i\omega t}$ , they form waves that are localized to the interface, either as standing waves or as waves that travel in vertical direction. They are called surface waves or surface plasmons.

Let us consider a silver foil with grating as indicated in the right part of Figure 9 and in Figure 10, dark regions define the set  $\Sigma_\eta$  which is occupied by silver, white regions are occupied by air. The mathematical problem reads as

follows: Let the permittivity be given, for some relative permittivity  $\varepsilon_r \in \mathbb{C}$ , by

$$\varepsilon_\eta(x) = \begin{cases} \varepsilon_r \eta^{-2} & \text{for } x \in \Sigma_\eta, \\ 1 & \text{for } x \notin \Sigma_\eta. \end{cases}$$

In particular,  $\varepsilon_\eta$  is large (in absolute value) in the metal part  $\Sigma_\eta$ . With this coefficient function, let  $u^\eta$  be a sequence of solutions to the Helmholtz problem

$$-\nabla \cdot \left( \frac{1}{\varepsilon_\eta} \nabla u^\eta \right) = \omega^2 u^\eta \quad \text{in } \Omega. \quad (24)$$

We assume that  $u^\eta \rightharpoonup u$  as  $\eta \rightarrow 0$  holds in  $L^2(\Omega)$  for some limit function  $u$  and ask: What is the equation for  $u$ ? Does the limit system explain the high transmission property of the silver foil?

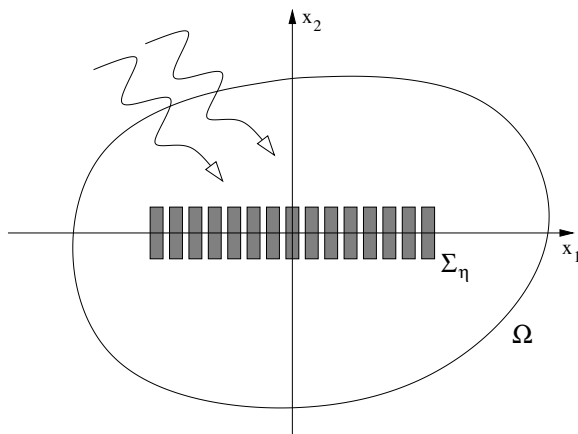


Figure 10: The transmission problem of a silver foil with a sub-wavelength grating. The height  $h$  of the silver foil is fixed in the limit process  $\eta \rightarrow 0$ , the channels have the width  $\alpha\eta$ , the periodicity of the channel structure is  $\eta$ .

These questions were answered in [16]. The effective system is

$$-\nabla \cdot (\hat{a} \nabla U) = \omega^2 \hat{\mu} U \quad \text{in } \Omega, \quad (25)$$

where  $\hat{a}(x) = a_{\text{eff}}$  and  $\hat{\mu}(x) = \mu_{\text{eff}}$  holds for  $x$  in the domain containing the meta-material,  $\hat{a}(x) = \hat{\mu}(x) = 1$  else. Once more, the variable  $U$  is *not* the weak limit of  $u^\eta$ , but it describes the typical value of  $u^\eta$  outside the metal. This is as in the above examples: In (13),  $v$  is the typical value of  $u^\varepsilon$  outside the resonators. In (17)–(18),  $\hat{H}$  is the typical value of  $H^\eta$  outside the resonators.

The coefficients of (25) can be calculated explicitly, they are  $a_{\text{eff}} = \begin{pmatrix} 0 & 0 \\ 0 & \alpha \end{pmatrix}$  and  $\mu_{\text{eff}} = \beta$ . The two tensors are determined by cell-problems which can, in this special case, be solved explicitly. The only nontrivial entry of  $a_{\text{eff}}(x)$  is given by  $\alpha > 0$ , the relative slit opening. The number  $\beta \in \mathbb{C}$  is the average of a shape

function. It can be expressed in terms of the geometrical quantities  $\alpha > 0$  and  $\gamma = (1 - \alpha)/2$ , and the physical quantities  $\omega > 0$  (frequency) and  $\varepsilon_r = -\sigma^2$  (we use this sign convention since we are particularly interested in negative values of  $\varepsilon_r$ ):

$$\beta = \frac{2 \sinh(\omega\sigma\gamma)}{\omega\sigma \cosh(\omega\sigma\gamma)} + \alpha \in \mathbb{C}.$$

For a real permittivity,  $\varepsilon_r \in \mathbb{R}$ , the number  $\sigma = \sqrt{-\varepsilon_r}$  is either real or imaginary. In both cases,  $\beta$  is real (it is the average of a real-valued solution to a cell-problem). But only for negative permittivity ( $\varepsilon_r < 0$  and  $\sigma \in \mathbb{R}$ ), the value of  $\beta$  stabilizes for large frequencies,  $\beta \rightarrow \alpha$  as  $\omega \rightarrow \infty$ .

## 4.2 Effective transmission system

Why can the effective system (25) imply interesting transmission properties? If  $\beta$  is a positive real number, the function  $U(x_2) = \sin(kx_2)$  can be a solution to (25) in the domain of the silver foil. Indeed, for the wave number  $k = \omega\sqrt{\beta/\alpha}$ , the relation  $\alpha k^2 = \omega^2\beta$  is satisfied and  $U$  solves  $\alpha U'' + \omega^2\beta U = 0$ .

Let us now study what happens when the frequency  $\omega$  is varied. If the relation  $kh \in \pi\mathbb{N}$  is satisfied for the height  $h$  of the foil, then the above function  $U$  is not only a solution to (25) in the silver foil, but it also vanishes on the upper and on the lower boundary. If this is the case, the silver foil supports an oscillatory solution, it is in resonance with  $\omega$ . As noted above, for  $\varepsilon_r < 0$  and  $\sigma \in \mathbb{R}$ ,  $\beta$  stabilizes for large frequencies. In this case, there are infinitely many solutions  $\omega$  to the relation  $\omega h\sqrt{\beta/\alpha} \in \pi\mathbb{N}$ , and these solutions have approximately a constant distance  $\pi/(h\sqrt{\beta/\alpha})$  (compare the right part of Figure 11 for the periodic pattern of maxima).

The (macroscopic) resonance of the silver foil couples the upper and the lower boundary and makes perfect transmission possible. To quantify transmission effects, the method of transfer matrices is used: Making an ansatz with incoming, reflected, and transmitted waves (compare the sketch of Figure 11), one calculates a transmission coefficient  $T \in \mathbb{C}$ , where  $|T| = 1$  implies perfect transmission. Denoting the angle of incidence by  $\theta \in (-\pi/2, \pi/2)$  ( $\theta = 0$  for normal incidence) and setting  $\tau = \sqrt{\beta/\alpha}$ , there holds

$$T = \left( \cos(\tau\omega h) - \frac{i}{2} \left[ \frac{\alpha\tau}{\cos(\theta)} + \frac{\cos(\theta)}{\alpha\tau} \right] \sin(\tau\omega h) \right)^{-1}. \quad (26)$$

The formula shows that, for  $\omega$  satisfying  $\sin(\tau\omega h) = 0$ , we have  $|T| = 1$  and hence perfect transmission. The result quantifies the perfect transmission effect and confirms our interpretation of the effect as a resonance of the surface plasmons with the macroscopic parameters  $h$  (height) and  $\omega$  (frequency).

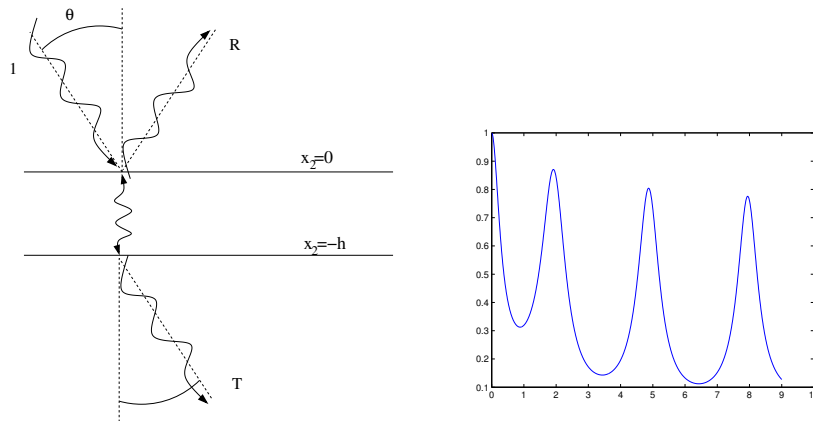


Figure 11: Transmission properties of the effective system. Left: The idea for the construction of the transmission coefficient  $T \in \mathbb{C}$ . The interface conditions for harmonic waves in the three subregions determine  $T$ . Right: The amplitude of transmission  $|T|$  in dependence of the frequency  $\omega$ . We used the physical and geometrical parameters of an experiment with silver. The figure shows  $|T|$  in dependence of  $\omega$  for the non-dimensionalized frequency.

## References

- [1] Allaire, G.: Homogenization and two-scale convergence. *SIAM J. Math. Anal.* **23**(6), 1482–1518 (1992)
- [2] Allaire, G.: Dispersive limits in the homogenization of the wave equation. *Ann. Fac. Sci. Toulouse Math.* (6) **12**(4), 415–431 (2003)
- [3] Allaire, G., Briane, M.: Multiscale convergence and reiterated homogenisation. *Proc. Roy. Soc. Edinburgh Sect. A* **126**(2), 297–342 (1996)
- [4] Allaire, G., Conca, C.: Bloch wave homogenization and spectral asymptotic analysis. *J. Math. Pures Appl.* (9) **77**(2), 153–208 (1998). DOI 10.1016/S0021-7824(98)80068-8
- [5] Allaire, G., Piatnitski, A.: Homogenization of nonlinear reaction-diffusion equation with a large reaction term. *Ann. Univ. Ferrara Sez. VII Sci. Mat.* **56**(1), 141–161 (2010). DOI 10.1007/s11565-010-0095-z
- [6] Beale, J.T.: Scattering frequencies of resonators. *Comm. Pure Appl. Math.* **26**, 549–563 (1973)
- [7] Bellieud, M., Bouchitté, G.: Homogenization of elliptic problems in a fiber reinforced structure. Nonlocal effects. *Ann. Scuola Norm. Sup. Pisa Cl. Sci.* (4) **26**(3), 407–436 (1998)
- [8] Bouchitté, G., Bellieud, M.: Homogenization of a soft elastic material reinforced by fibers. *Asymptot. Anal.* **32**(2), 153–183 (2002)

- [9] Bouchitté, G., Bourel, C., Felbacq, D.: Homogenization of the 3D Maxwell system near resonances and artificial magnetism. *C. R. Math. Acad. Sci. Paris* **347**(9-10), 571–576 (2009). DOI 10.1016/j.crma.2009.02.027
- [10] Bouchitté, G., Felbacq, D.: Low frequency scattering by a set of parallel metallic rods. In: *Mathematical and numerical aspects of wave propagation* (Santiago de Compostela, 2000), pp. 226–230. SIAM, Philadelphia, PA (2000)
- [11] Bouchitté, G., Felbacq, D.: Homogenization near resonances and artificial magnetism from dielectrics. *C. R. Math. Acad. Sci. Paris* **339**(5), 377–382 (2004). DOI 10.1016/j.crma.2004.06.018
- [12] Bouchitté, G., Felbacq, D.: Left handed media and homogenization of photonic crystals. *Optics letters* **30**(159, 10.1088), 1189–1191. (2005)
- [13] Bouchitté, G., Felbacq, D.: Negative refraction in periodic and random photonic crystals. *New J. Phys* **7**(159, 10.1088) (2005)
- [14] Bouchitté, G., Felbacq, D.: Homogenization of a wire photonic crystal: the case of small volume fraction. *SIAM J. Appl. Math.* **66**(6), 2061–2084 (2006)
- [15] Bouchitté, G., Schweizer, B.: Homogenization of Maxwell’s equations in a split ring geometry. *Multiscale Model. Simul.* **8**(3), 717–750 (2010). DOI 10.1137/09074557X
- [16] Bouchitté, G., Schweizer, B.: Plasmonic waves allow perfect transmission through sub-wavelength metallic gratings. *Netw. Heterog. Media* **8**(4), 857–878 (2013). DOI 10.3934/nhm.2013.8.857
- [17] Brown, R., Hislop, P.D., Martinez, A.: Eigenvalues and resonances for domains with tubes: Neumann boundary conditions. *J. Differential Equations* **115**(2), 458–476 (1995). DOI 10.1006/jdeq.1995.1023
- [18] Cao, Q., Lalanne, P.: Negative role of surface plasmons in the transmission of metallic gratings with very narrow slits. *Phys. Rev. Lett.* **88**, 057,403 (2002). DOI 10.1103/PhysRevLett.88.057403
- [19] Chen, Y., Lipton, R.: Resonance and double negative behavior in metamaterials. *Arch. Ration. Mech. Anal.* **209**(3), 835–868 (2013). DOI 10.1007/s00205-013-0634-8
- [20] Cherednichenko, K.D., Smyshlyaev, V.P., Zhikov, V.V.: Non-local homogenized limits for composite media with highly anisotropic periodic fibres. *Proc. Roy. Soc. Edinburgh Sect. A* **136**(1), 87–114 (2006). DOI 10.1017/S0308210500004455

- [21] Cherednichenko, K.D., Smyshlyaev, V.P., Zhikov, V.V.: Non-local homogenized limits for composite media with highly anisotropic periodic fibres. *Proc. Roy. Soc. Edinburgh Sect. A* **136**(1), 87–114 (2006)
- [22] Cioranescu, D., Damlamian, A., Griso, G.: Periodic unfolding and homogenization. *C. R. Math. Acad. Sci. Paris* **335**(1), 99–104 (2002). DOI 10.1016/S1631-073X(02)02429-9
- [23] Dohnal, T., Lamacz, A., Schweizer, B.: Bloch-wave homogenization on large time scales and dispersive effective wave equations. *Multiscale Model. Simul.* **12**(2), 488–513 (2014). DOI 10.1137/130935033
- [24] Felbacq, D., Bouchitté, G.: Homogenization of a set of parallel fibres. *Waves Random Media* **7**(2), 245–256 (1997)
- [25] Fernández, C., Menzala, G.P.: Resonances of an elastic resonator. *Appl. Anal.* **76**(1-2), 41–49 (2000). DOI 10.1080/00036810008840864
- [26] Gadyl'shin, R.R.: On analogues of the Helmholtz resonator in averaging theory. *Mat. Sb.* **193**(11), 43–70 (2002). DOI 10.1070/SM2002v193n11ABEH000691
- [27] Gadyl'shin, R.R.: On domains with a narrow isthmus in the critical case. *Proc. Steklov Inst. Math. (Asymptotic Expansions. Approximation Theory. Topology, suppl. 1)*, S68–S74 (2003)
- [28] Holloway, C.L., Kuester, E.F., Baker-Jarvis, J., Kabos, P.: A double negative (dng) composite medium composed of magnetodielectric spherical particles embedded in a matrix. *IEEE Transactions on Antennas and Propagation* **51**(10), 2596–2603 (2003). DOI 10.1109/TAP.2003.817563
- [29] Jikov, V.V., Kozlov, S.M., Oleĭnik, O.A.: Homogenization of differential operators and integral functionals. Springer-Verlag, Berlin (1994). Translated from the Russian by G. A. Yosifian [G. A. Iosifyan]
- [30] Joly, P., Tordeux, S.: Asymptotic analysis of an approximate model for time harmonic waves in media with thin slots. *M2AN Math. Model. Numer. Anal.* **40**(1), 63–97 (2006). DOI 10.1051/m2an:2006008
- [31] Joly, P., Tordeux, S.: Matching of asymptotic expansions for waves propagation in media with thin slots. II. The error estimates. *M2AN Math. Model. Numer. Anal.* **42**(2), 193–221 (2008). DOI 10.1051/m2an:2008004
- [32] Kohn, R., Shipman, S.: Magnetism and homogenization of micro-resonators. *Multiscale Modeling & Simulation* **7**(1), 62–92 (2007)



- [33] Lamacz, A., Schweizer, B.: Effective Maxwell equations in a geometry with flat rings of arbitrary shape. *SIAM J. Math. Anal.* **45**(3), 1460–1494 (2013). DOI 10.1137/120874321
- [34] Lamacz, A., Schweizer, B.: Effective acoustic properties of a meta-material consisting of small Helmholtz resonators. *DCDS-S* (2016)
- [35] Lamacz, A., Schweizer, B.: A negative index meta-material for Maxwell’s equations. *SIAM J. Math. Anal.* (2016). (in press)
- [36] Lipton, R., Schweizer, B.: Negative magnetic response in a material with perfectly conducting split rings. in preparation (2016)
- [37] Milton, G.W.: Realizability of metamaterials with prescribed electric permittivity and magnetic permeability tensors. *New Journal of Physics* **12**(3), 033,035 (2010)
- [38] Nguetseng, G.: A general convergence result for a functional related to the theory of homogenization. *SIAM J. Math. Anal.* **20**(3), 608–623 (1989). DOI 10.1137/0520043
- [39] O’Brien, S., Pendry, J.: Magnetic activity at infrared frequencies in structured metallic photonic crystals. *J. Phys. Condens. Mat.* **14**, 6383 – 6394 (2002)
- [40] Pendry, J.: Negative refraction makes a perfect lens. *Phys. Rev. Lett.* **85**(3966) (2000)
- [41] Porto, J.A., Garcia-Vidal, F.J., Pendry, J.B.: Transmission resonances on metallic gratings with very narrow slits. *Phys. Rev. Lett.* **83**, 2845–2848 (1999). DOI 10.1103/PhysRevLett.83.2845
- [42] Sánchez-Palencia, E.: Nonhomogeneous media and vibration theory, *Lecture Notes in Physics*, vol. 127. Springer-Verlag, Berlin (1980)
- [43] Schweizer, B.: The low-frequency spectrum of small Helmholtz resonators. *Proc. A.* **471**(2174), 20140,339, 18 (2015). DOI 10.1098/rspa.2014.0339
- [44] Shelby, R.A., Smith, D.R., Schultz, S.: Experimental verification of a negative index of refraction. *Science* **292**(5514), 77–79 (2001). DOI 10.1126/science.1058847
- [45] Smith, D., Pendry, J., Wiltshire, M.: Metamaterials and negative refractive index. *Science* **305**, 788–792 (2004)
- [46] Veselago, V.: The electrodynamics of substances with simultaneously negative values of  $\epsilon$  and  $\mu$ . *Soviet Physics Uspekhi* **10**, 509–514 (1968)

## Preprints ab 2013/08

- 2016-04 **Ben Schweizer**  
Resonance meets homogenization - Construction of meta-materials with astonishing properties
- 2016-03 **Ben Schweizer**  
On Friedrichs inequality, Helmholtz decomposition, vector potentials, and the div-curl lemma
- 2016-02 **Michael Voit**  
Generalized commutative association schemes, hypergroups, and positive product formulas
- 2016-01 **Agnes Lamacz and Ben Schweizer**  
Effective acoustic properties of a meta-material consisting of small Helmholtz resonators
- 2015-13 **Christian Eggert, Ralf Gäer, Frank Klinker**  
The general treatment of non-symmetric, non-balanced star circuits: On the geometrization of problems in electrical metrology
- 2015-12 **Daniel Kobe and Jeannette H.C. Woerner**  
Oscillating Ornstein-Uhlenbeck processes and modelling electricity prices
- 2015-11 **Sven Glaser**  
A distributional limit theorem for the realized power variation of linear fractional stable motions
- 2015-10 **Herold Dehling, Brice Franke and Jeannette H.C. Woerner**  
Estimating drift parameters in a fractional Ornstein Uhlenbeck process with periodic mean
- 2015-09 **Harald Garcke, Johannes Kampmann, Andreas Rätz and Matthias Röger**  
A coupled surface-Cahn-Hilliard bulk-diffusion system modeling lipid raft formation in cell membrans
- 2015-08 **Agnes Lamacz and Ben Schweizer**  
Outgoing wave conditions in photonic crystals and transmission properties at interfaces
- 2015-07 **Manh Hong Duong, Agnes Lamacz, Mark A. Peletier and Upanshu Sharma**  
Variational approach to coarse-graining of generalized gradient flows
- 2015-06 **Agnes Lamacz and Ben Schweizer**  
A negative index meta-material for Maxwell's equations
- 2015-05 **Michael Voit**  
Dispersion and limit theorems for random walks associated with hypergeometric functions of type  $BC$
- 2015-04 **Andreas Rätz**  
Diffuse-interface approximations of osmosis free boundary problems
- 2015-03 **Margit Rösler and Michael Voit**  
A multivariate version of the disk convolution
- 2015-02 **Christina Dörlemann, Martin Heida, Ben Schweizer**  
Transmission conditions for the Helmholtz-equation in perforated domains
- 2015-01 **Frank Klinker**  
Program of the International Conference  
Geometric and Algebraic Methods in Mathematical Physics  
March 16-19, 2015, Dortmund

- 2014-10 **Frank Klinker**  
An explicit description of  $SL(2, \mathbb{C})$  in terms of  $SO^+(3, 1)$  and vice versa
- 2014-09 **Margit Rösler and Michael Voit**  
Integral representation and sharp asymptotic results for some Heckman-Opdam hypergeometric functions of type BC
- 2014-08 **Martin Heida and Ben Schweizer**  
Stochastic homogenization of plasticity equations
- 2014-07 **Margit Rösler and Michael Voit**  
A central limit theorem for random walks on the dual of a compact Grassmannian
- 2014-06 **Frank Klinker**  
Eleven-dimensional symmetric supergravity backgrounds, their geometric superalgebras, and a common reduction
- 2014-05 **Tomáš Dohnal and Hannes Uecker**  
Bifurcation of nonlinear Bloch waves from the spectrum in the Gross-Pitaevskii equation
- 2014-04 **Frank Klinker**  
A family of non-restricted  $D = 11$  geometric supersymmetries
- 2014-03 **Martin Heida and Ben Schweizer**  
Non-periodic homogenization of infinitesimal strain plasticity equations
- 2014-02 **Ben Schweizer**  
The low frequency spectrum of small Helmholtz resonators
- 2014-01 **Tomáš Dohnal, Agnes Lamacz, Ben Schweizer**  
Dispersive homogenized models and coefficient formulas for waves in general periodic media
- 2013-16 **Karl Friedrich Siburg**  
Almost opposite regression dependence in bivariate distributions
- 2013-15 **Christian Palmes and Jeannette H. C. Woerner**  
The Gumbel test and jumps in the volatility process
- 2013-14 **Karl Friedrich Siburg, Katharina Stehling, Pavel A. Stoimenov, Jeannette H. C. Wörner**  
An order for asymmetry in copulas, and implications for risk management
- 2013-13 **Michael Voit**  
Product formulas for a two-parameter family of Heckman-Opdam hypergeometric functions of type BC
- 2013-12 **Ben Schweizer and Marco Veneroni**  
Homogenization of plasticity equations with two-scale convergence methods
- 2013-11 **Sven Glaser**  
A law of large numbers for the power variation of fractional Lévy processes
- 2013-10 **Christian Palmes and Jeannette H. C. Woerner**  
The Gumbel test for jumps in stochastic volatility models
- 2013-09 **Agnes Lamacz, Stefan Neukamm and Felix Otto**  
Moment bounds for the corrector in stochastic homogenization of a percolation model
- 2013-08 **Frank Klinker**  
Connections on Cahen-Wallach spaces